Fractal Laws for Spatial and Temporal Variables of Brittle Fragmentation

Davydova M. [1,a] , Uvarov S. [2,b]

[1] ICMM UB RAS, 1, Ac. Korolev str., 614013 Perm, Russia

[2] ICMM UB RAS, 1, Ac. Korolev str., 614013 Perm, Russia

[a] davydova@icmm.ru, [b] usv@icmm.ru

Keywords: Fragmentation, scaling, self-organized criticality.

Abstract. The study of fragmentation statistics of brittle materials that includes four types of experiments is presented. Data processing of the fragmentation of glass plates under quasi-static loading and the fragmentation of quartz cylindrical rods under dynamic loading shows that the size distribution of fragments (spatial quantity) is fractal and can be described by a power law. The original experimental technique allows us to measure, apart from the spatial quantity, the temporal quantity - the size of the time interval between the impulses of intensive light emission (mechanoluminescence or fractoluminescence). The analysis of distributions of spatial (fragment size) and temporal (time interval) quantities provides evidence of obeying scaling laws, which suggests the possibility of self-organized criticality in fragmentation.

Introduction

Fragmentation, the process of breaking solids into separate fragments, is caused by multiple fractures and can be observed in both engineering and natural objects over a wide range of spatial and temporal scales. An investigation of fragmentation statistics usually includes the determination of the cumulative distribution of fragment sizes or masses, i.e., the number of fragments $N(m)$ with a size or mass larger than s or m, respectively. The distribution type depends on loading conditions, material characteristics and sample geometries. Many types of distribution functions have been observed experimentally: log-normal, power-law, Mott, exponential, Weibull, and combined exponential and power-law [1,2,3,4,5,6,7,8,9,10]. Summarizing the results of experimental data processing, we can classify all these distribution functions into two groups: exponential and power law. The assumption that the exponential distribution is typical of the fragmentation of ductile materials and the power-law distribution characterizes brittle fragmentation has been discussed by Grady [7]. Donald Turcotte [8] has pursued the fragmentation of brittle materials as a fractal process resulting in the power law distribution function $N \sim x^{-d}$, where N is the number of fragments, x is the linear dimension of fragments, and d is the fractal dimension. The fractal character of the distribution function in a wide range of fragment sizes has led Oddershede et al. [3] to suppose that the fragmentation exhibits self-organized criticality (SOC). In their seminal paper Per Bak, Chao Tang and Kurt Wiesenfeld [11] have put forward a new concept of SOC and carried out numerical simulation, which enables the description of the behavior of a sand pile (example of a self-organized critical system) and leads to the following conclusions:

- distribution of the life times of avalanches obeys a power law;
- distribution of the avalanche sizes follows a power law as well.

In other words, to prove that the system exhibits SOC, it is necessary to establish the existence of a power law for temporal and spatial quantities. The purpose of this experimental study is to

demonstrate that the fragmentation process exhibits SOC. To this end, we need to determine the distribution of temporal and spatial variables.

Fragmentation of Glass Plates under Quasi-Static Loading

Quasi-static testing was performed in the experiments with glass plates loaded in a "sandwich" to save the glass fragmentation pictures (Fig. 1a). Using the original software, the images were

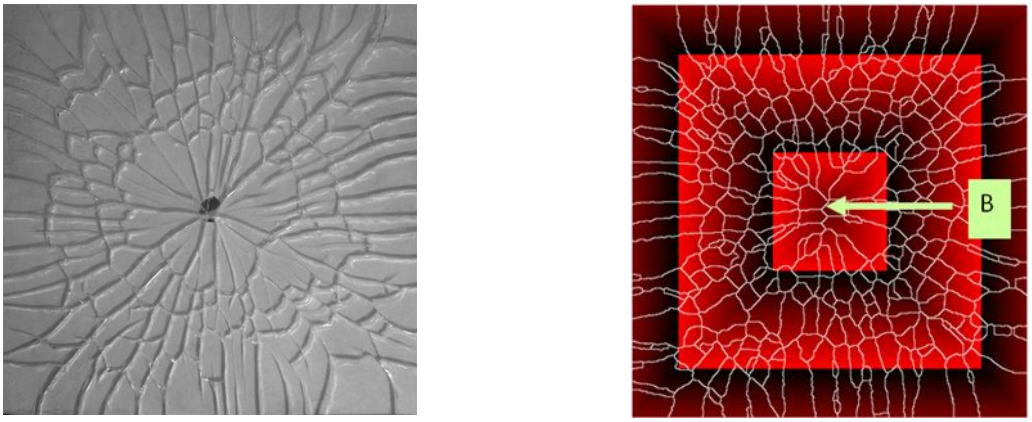

a) b)

Fig. 1. a) Photographs of typical fragmentation patterns. b) Schematic pictures of fragmentation patterns to determine the size and number of fragments and the total length of cracks.

transformed into the schematic pictures corresponding to the fragmentation patterns (Fig. 1b). This made it possible to determine the size and number of fragments and the total length of cracks. We consider two types of scaling. The first type is based on the relation

$$L(r) \sim r^{D}, \qquad (1)$$

where $L(r)$ is the total crack length in the boxes of a size $r \times r$ centred at the point B (Fig. 1b), and D is the fractal dimension. The second type is the traditional definition of the cumulative distribution of fragment sizes, that is, the calculation of the number of fragments $N(s)$ with a size larger than S.

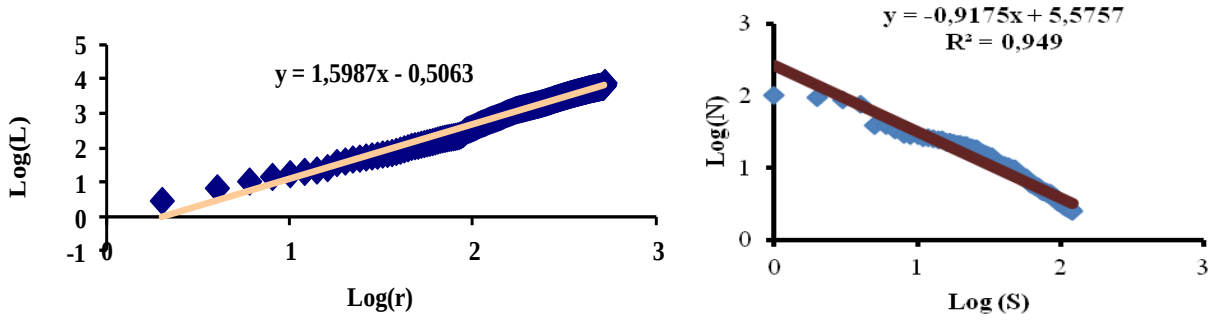

a) b)

Fig. 2. a) Scaling law obtained using the relation for crack length (1). b) Cumulative log-log plots of the fragments size distributions.

The use of expression (1) was discussed by Sornette et al. [12]. However, it should be noted that the fracture pattern [12] does not have a distinct central point. At the same time, the examined fragmentation patterns have a central point, and their configuration is similar to that created with the model of diffusion-limited aggregation (DLA) [13] or the model of dielectric breakdown (DB) [14]. Relation (1) can be used to define the fractal dimension for both these models. In the case of the DB model, $L(r)$ is the total length of the discharge branches within the circle of radius r For the DLA model, $L(r)$ is the number of particles. By analogy with the DLA and DB models, to determine the fractal dimension of the fragmentation patterns, we use relation (1), where $L(r)$ is the total length of cracks in the boxes of a size $r \times r$ centred at the point B (Fig. 1b). The minimal number of the boxes used for calculation of the fractal dimension is 200. The scaling law obtained using the relation for crack length (1) is presented in Fig. 2a. The processing of the fragment sizes shows that the relation between the fragment area and the number is also fitted by a power law (Fig. 2b).

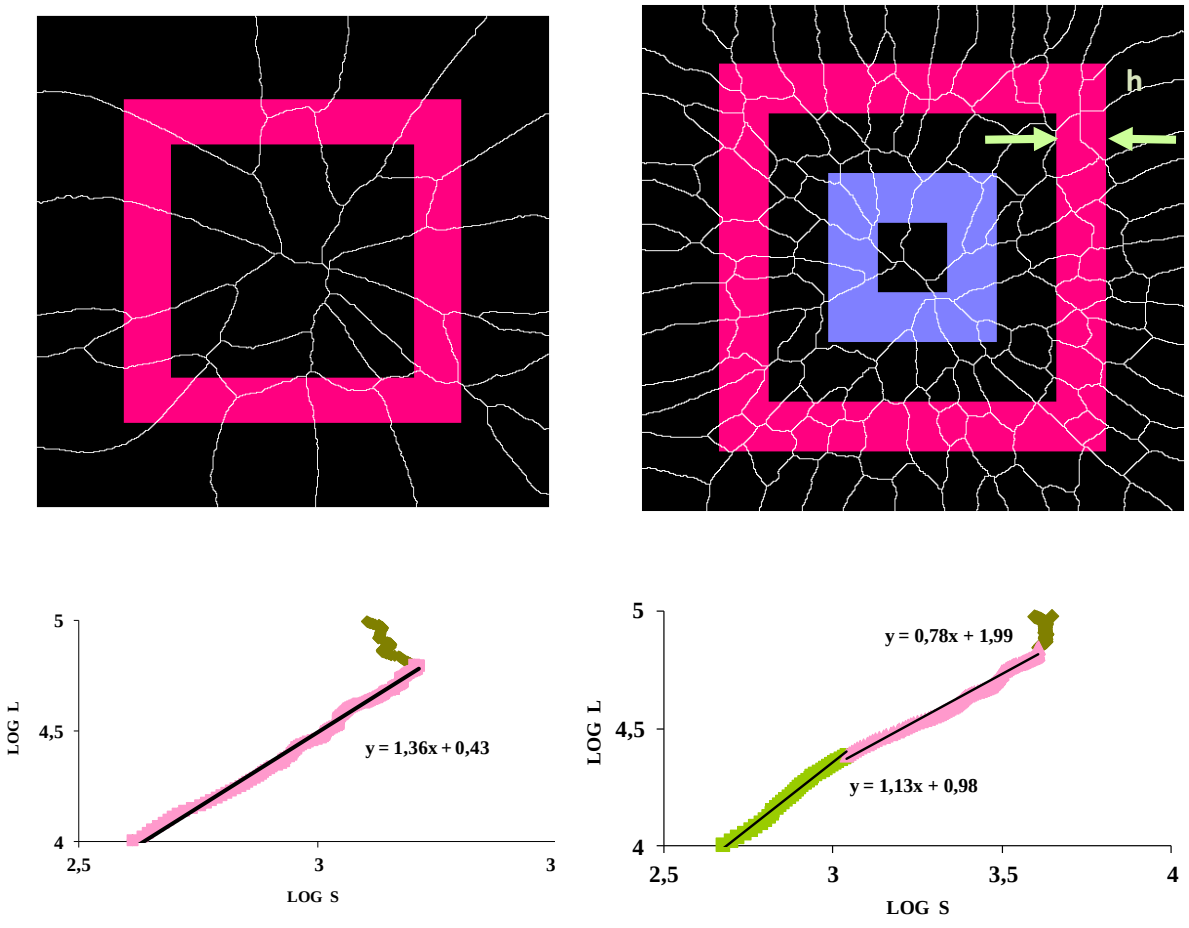

a) b)

Fig. 3. a) Fragmentation pattern and fractal dimension definition for the fracture accompanied by radial crack formation. b) Fragmentation pattern and fractal dimension definition for the fracture accompanied by a change in the fracture mechanism.

There are two types of energy-dependent fragmentation patterns leading to a breakup (Fig. 3). Fig. 3a presents a fragmentation pattern that illustrates the fracture accompanied by radial crack formation. The right fragmentation pattern (Fig. 3b) has two zones corresponding to two different fracture mechanisms. The central zone has a radial crack only. In the second zone, the crack

branching process is observed. Assuming that different fracture mechanisms characterize different fractal dimensions, we have

$$L(S) \sim S^D, \qquad (2)$$

where $L(S)$ is the total crack length inside the square frame with a thickness h (Fig. 3a), S is the frame area, and D is the fractal dimension. Calculation the fractal dimension using expression (2) shows that, for the left fragmentation pattern (Fig. 3a), the data is fitted by a single line. For the right pattern, the log-log representation of $L(S)$ changes its slope, and the power-law exponent D decreases. A change in the fracture mechanism (from radial crack formation to crack branching) correlates with the qualitative changes in the fractal dimension.

Fragmentation of Quartz Rods under Dynamic Loading

As shown in the section "Introduction", to confirm the fact that the fragmentation exhibits SOC, we need to establish the existence of a power law for temporal and spatial quantities. For this purpose, the fragmentation statistics has been studied in the recovery dynamic experiments with quartz cylindrical rods using a ballistic set-up (Fig.4). We have concentrated on the determination of:

- fragment size distribution;
- distribution of the time interval between the impulses of intensive light emission (mechanoluminescence or fractoluminescence).

At the first stage of the experiment, the main goal was to evaluate the effect of loading conditions and the shape and size of the sample on the fragment size distribution function. Three types of loading conditions (I, II, III) were realized using a ballistic set-up:

- fragmentation as a result of interaction of direct and reflected compression waves (I) (Fig.4a);
- fragmentation under the action of a compression wave (II) (Fig.4b);
- fragmentation induced by a direct compression wave and its reverberation in rod (III) (Fig.4c).

Loading Condition I. The ballistic set-up consists of a gas gun with a bore of 19.3 mm diameter, a velocity registration system and a base where the sample is mounted (Fig. 4a). The sectional glass rod is composed of a buffer and the main part covered by an elastic shell. The buffer was used for realization of uniaxial loading produced by a cylindrical projectile of mass 13.9 g accelerated up to the velocities of 6-22 m/s.

Loading Condition II. To avoid the possible influence of the reflected wave on the fragmentation scenario, the ballistic set-up was modified. The sample was placed into a steel cylinder filled with plastic foam (Fig. 4b). The sectional glass rod was composed of a buffer, main part and outer parts. The presence of the last part made it possible to catch the reflected wave.

Loading Condition III. The scheme given in Fig. 4c illustrates the experimental technique used to measure the distribution of time quantities. Impact leads to the formation of fracture surfaces, which produce intensive light emission (mechanoluminescence or fractoluminescence).The intensity of the light is registered by the Photo Multiplayer Tube connected with the oscilloscope (oscilloscope sample rate is 1 GHz).

Definition of Fragment Mass Distribution. The mass of the fragments passing through the sieves was obtained by weighting the fragments using an electronic balance HR-202i (accuracy 10^{-4} g). The mass of the fragments corresponding to the maximum of the probability density function varied in the range from $2*10^{-4}$g to $6*10^{-4}$ g (Fig.5a). The cumulative fragment size distribution, i.e. the number of fragments *N(m)* with a mass greater than a specified value *m*, was fitted by the power law (Fig.5b). The fragmentation statistics was analyzed by varying the sample size and load intensity (projectile velocity). The results of experiments have indicated that the variation in the sample size and loading conditions does not lead to the change in the probability density function and

cumulative mass distribution. The mass of the fragments corresponding to the maximum of the probability density function is independent of the projectile energy (Fig. 5).

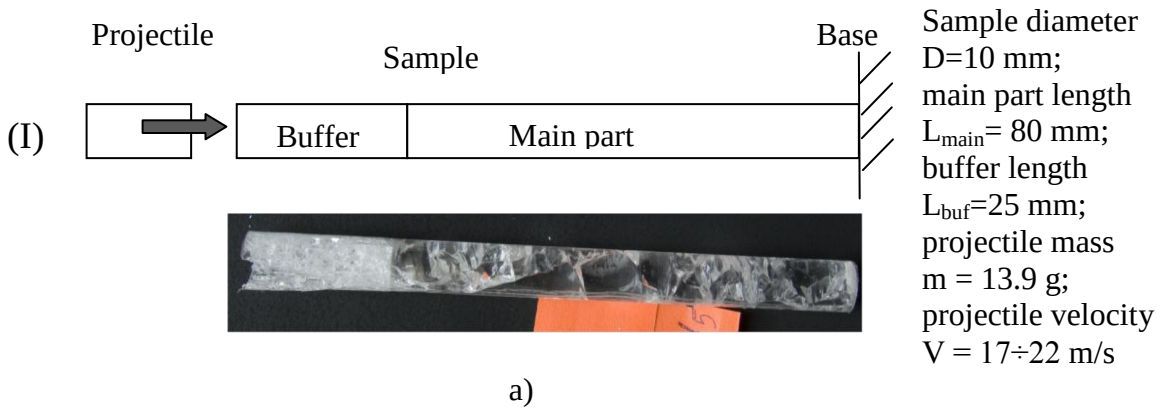

a)

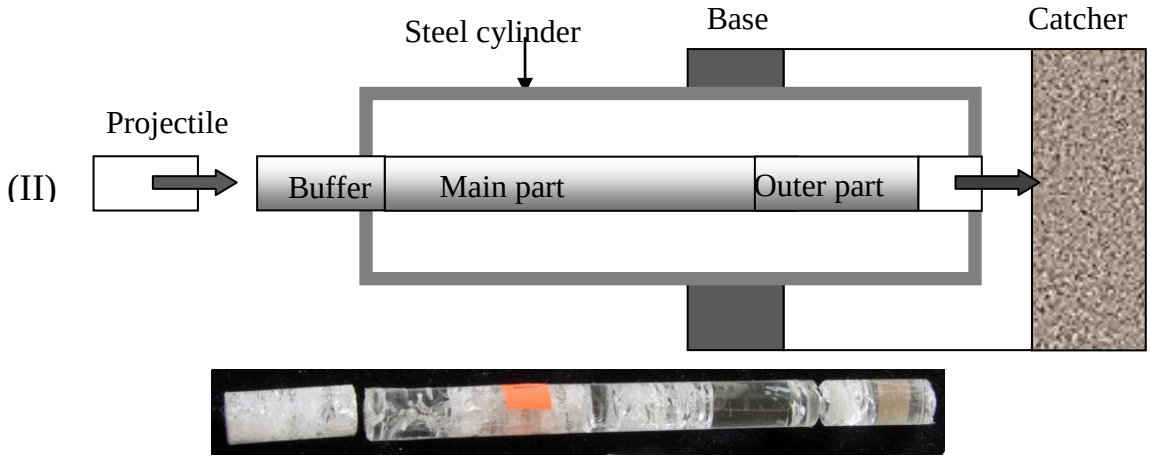

Sample diameter D=12 mm; main part length L_{main} = 120 mm; buffer length L_{buf} =25 mm; outer part length L_{out}= 30 мм; projectile mass m = 6.3 g; V = 40÷50 m/s

b)

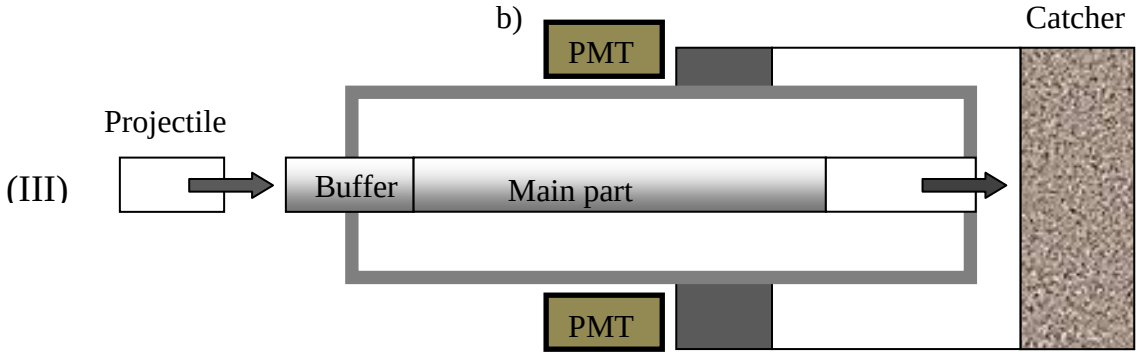

Sample diameter D=12 mm; main part length L_{main} = 120 mm; buffer length L_{buf} =25 мм;

c)

Fig. 4. Schemes of loading: a) condition I; b) condition II; c) condition III.

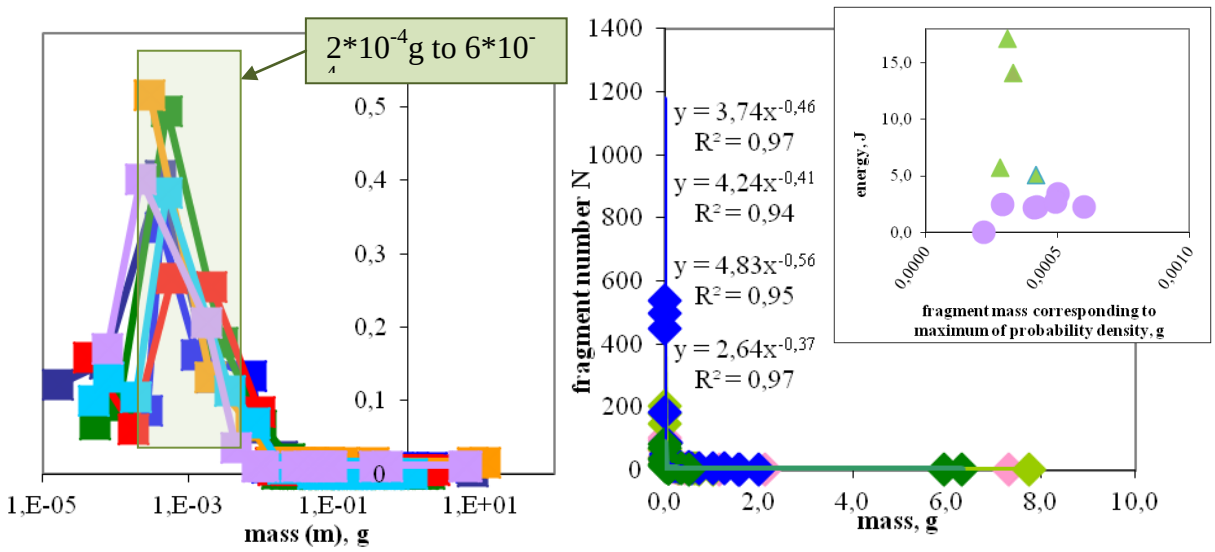

Fig.5. a) Probability density function. b) Cumulative fragment size distribution. The plot in the upper right-hand corner illustrates the dependence of fragment mass on the projectile energy.

Thus, the cumulative distributions illustrating the relation between the numbers of fragments and their linear dimension are represented as a log-log plot (Fig. 6). The linear dimension is defined as a cube root of mass or a square root of area. The distribution is fractal by nature with a power law in the form $N(>r) = Cr^{-D}$, where N is the number of fragments with a characteristic linear dimension greater than r. The fractal dimension D varies from 1.6 to 2.0 for the plate and from 1.1 to 1.7 for the rod (Loading Conditions I and II).

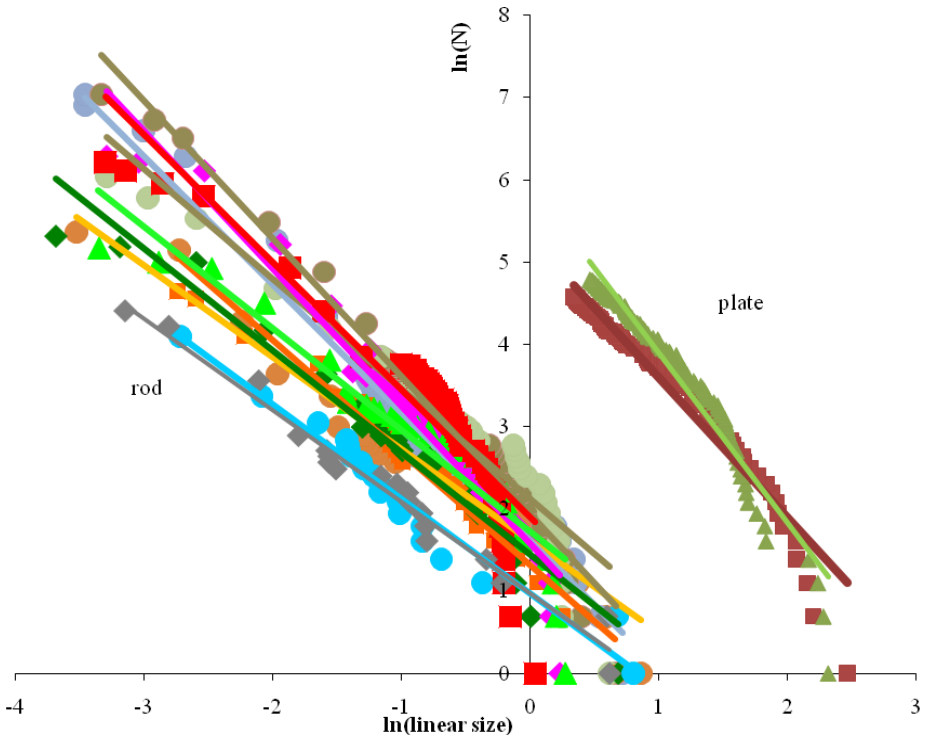

Fig. 6. Double logarithmic plot of the cumulative distribution function for plate and rod.

Definition of Distribution of Time Interval between the Impulses of Intensive Light Emission. To measure the scaling of spatial and time quantities corresponding to the same sample, we have developed the experimental scheme presented in Fig.4c (Loading Condition III). Fracture surfaces formed under impact loading produced intensive light emission (mechanoluminescence or fractoluminescence). The mechanoluminescence impulses were registered by two PMT connected with the oscilloscope (Fig.7).

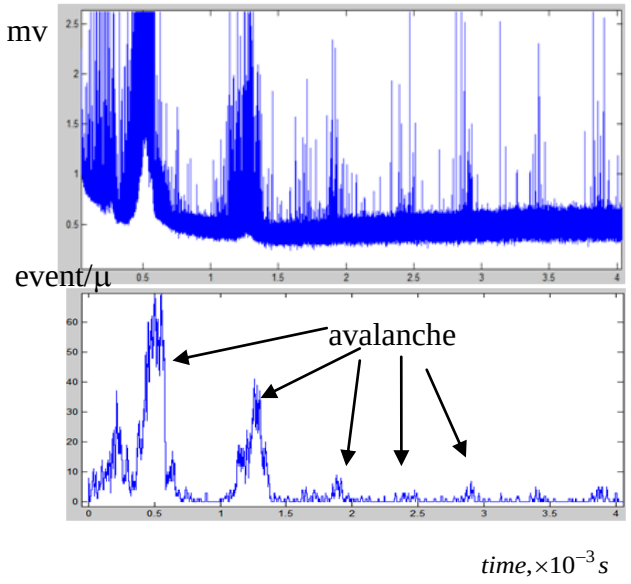

Fig. 7. Signal of the oscilloscope and the frequency of impulse appearance.

The process of light reflection looks like the process of avalanche spreading (Fig. 7). The lower plot represents the event frequency. The events are distributed in blocks.

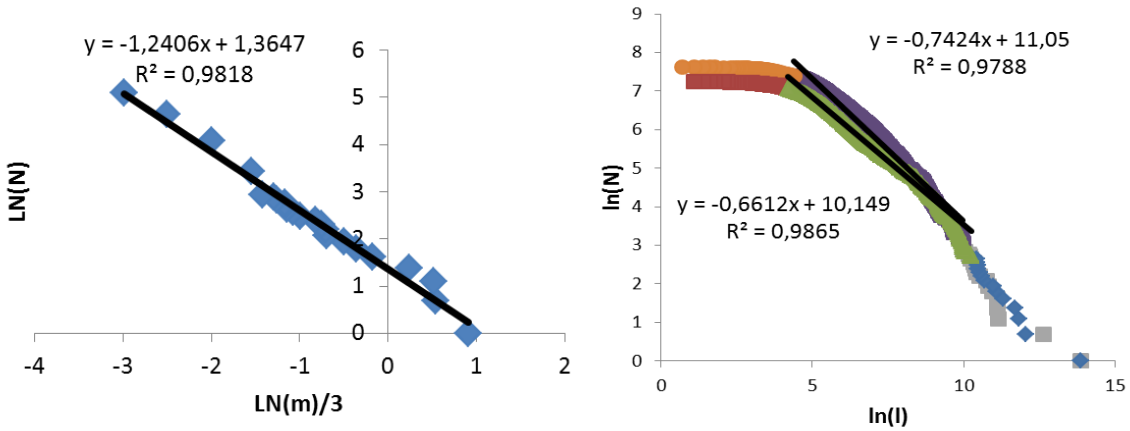

a) b)

Fig. 8. a) Fragment size distribution (spatial scaling). b) Distribution of time interval separating the fractoluminescence impulses.

The cumulative distribution function of the time interval (registered by two PMT) in the double logarithmic plot (Fig.8b) is fitted by the straight line (90% of the total number points). At small sizes

(8% of the total number of points), the curve deviates from the straight line because the size of time interval is comparable with the oscilloscope sample rate (1 GHz). The falloff at the largest interval sizes (2% of the total number of points) is due to finite-size effects. In this case, the time interval is comparable with the process time. The average exponent for the signals corresponding to two PMT placed near the opposite side of the sample is 0.7. The central part is the line covering 90% of the total number of points. It has been found that the fragment size distributions (Fig.8a) and the time interval distributions (Fig.8b) obey scaling laws, which suggests the possibility of self-organized criticality in fragmentation.

Conclusion.

Experimental investigations have been carried out to examine the fragmentation of brittle materials under quasi-static and dynamic loading conditions. Based on the obtained results, the following conclusions can be derived:

- fragmentation patterns of glass plates are fractal;
- variation in the fracture mechanism of plates correlates with the changes in the fractal dimension;
- fragment size distribution for the observed type of fragmentation is fractal and satisfies the relation $N(>r) = Cr^{-D}$;
- fragment size distributions and time interval distributions are governed by scaling laws, which is indicative of the self-organized critical behavior during the fragmentation process.

Acknowledgement. We are very grateful to Vladimir Leont'ev for help in performing experiments. The author would like to acknowledge the Russian Foundation for Basic Research (grant RFBR 11-01-96010, grant RFBR 11-01-00712).

References

[1] Grady, D.E.; Kipp, M.E.: J.Appl. Phys. Vol. 58, N 3 (1985), p.1210-1222.
[2] Kadono, T.: Phys. Rev. Letters Vol. 78, N 8 (1997), p.1444-1447.
[3] Oddershede, L.; Dimon, P.; Bohr, J.: Phys. Rev. Letters Vol. 71, N 19 (1993), p.3107-3110.
[4] Sil'vestrov, V. V.: Combustion, Explosion, and Shock Waves Vol. 40, N 2 (2004), p. 225–237.
[5] Weiss, J.: Engineering Fracture Mechanics Vol. 68 (2001), p.1975-2012.
[6] Emily S.C. Ching, S.L. Lui, Ke-Qing Xia: Physica A Vol. 287 (2000), p. 83 – 90.
[7] Grady, D.E.: International Journal of Fracture Vol. 153, N 1-2 (2010), p.85-99.
[8] Turcotte, D. L.: *Fractals and chaos in geology and geophysics* (Cambridge University Press, UK 1997).
[9] Hiroaki K. Satoshi I. and Haruo H.: Phys. Rev. Letters Vol. 95 (2005) p. 095503(1-4).
[10] Ishii, T., Matsushita, M.: J. Phys. Soc. Japan Vol. 61, (1992) p. 3474 -347.
[11] Bak, P.; Tang C.; Wiesenfeld, K.: Phys. Rev. Letters Vol. 59, N4, (1987), 381-384.
[12] Sornette, A.; Davy, P.; Sornette, D.: Phys. Rev. Letters Vol. 65, N18 (1990) p. 2266-2269.
[13] Niemeyer, L.; Pietronero L.; Wiesmann H.J.: Phys. Rev. Letters Vol. 52, N12, (1984) p.1033-1036.
[14] Witten T.A.; Sander L.M.: Phys. Rev. Letters Vol. 47, N19, (1981) p.1400-1403.